



Numerical Investigation of Flow Field around a Mannequin Model with Airway System in an Air Conditioned Room

M. Azhdari, M. M. Tavakol*

Department of Mechanical Engineering, Shiraz Branch, Islamic Azad University, Shiraz, Iran

ABSTRACT: In this study, air flow around a mannequin equipped with a respiratory system at the center of ventilated room was studied numerically. In the first mode the air conditioner dampers were installed on the front wall and in the second modes they were installed on the right side wall. The inhalation rates of 15, 20 and 30 lit/min were simulated from the nostril inlet to the end of trachea. Flow field including the region around mannequin and airway, integrally, was evaluated by solving the Navier-Stokes and continuity equations in steady state condition by means of $k-\omega$ -SST transition turbulence model in the Ansys-Fluent software. Pressure distribution, turbulence intensity, shear stress and streamlines were evaluated inside the airway passage. Furthermore, the velocity distribution and streamlines near the mannequin face for two ventilation modes were analyzed. According to the results for the turbulence intensity distribution the turbulent flow was observed inside the respiratory system for all of the breathing rates and location of the air condition dampers did not affect the turbulence intensity distribution inside the respiratory system. In addition, in the second mode, the lower air velocity was obtained around the mannequin face and better comfort condition inside the room was maintained.

Review History:

Received: 6 May. 2018
Revised: 14 July 2018
Accepted: 7 Sep. 2018
Available Online: 11 Sep. 2018

Keywords:

Mannequin
Respiratory system
Air conditioning
Inhalation flow rate

1. Introduction

Air conditioning systems should provide occupancy comfort condition. The installation location of inlet and outlet air-conditioning dampers may have considerable influence on the flow field. The air flow velocity and occupancy comfort condition are very important in building design. In the past studies, researchers have investigated the separated human respiratory system. They reported laminar flow condition in the nasal cavity for inhalation rates of 7.5 to 12 lit/min per each nostril and turbulent flow condition for inhalation flow rates of 12 to 38 lit/min for physical activities [1]. Cheng et al. [2] measured the pressure drop of the airway model of a normal human adult male from the nose to larynx at constant inspiration flow rates between 4 to 60 liter/minute by experimental study. Wen et al. [3] constructed the nasal cavity geometry from the Computerized Tomography Scan (CT Scan) image and evaluated the flow field inside the cavity. They compared their results for the right and left nasal cavity with available experimental and numerical data for the inspiration rates of 7.5 and 15 lit/min. Results showed that pressure drop in the right cavity is lower than the left one because of the larger cross-sectional area. Xi et al. [4] investigated the pressure drop of various models with different ages from nose inlet to larynx. They highlighted that for a specified activity the inspiration flow rate increases with

the age. They showed that in the same inspiration rates, the airway passage with higher hydraulic diameter corresponds to the lower pressure drop.

Some researchers have investigated the flow field of air in the room with or without mannequin. Rim and Novoselac [5] investigated the effect of the air conditioning system on the flow field inside a room experimentally and numerically. Se et al. [6] obtained the flow pattern in a room with a realistic human model and simulated the inspiration rates of 15 and 40 lit/min in the room. Zhang et al. [7] investigated the air flow in a room with inlet and outlet air-conditioning dampers and compared the results with experimental data.

Based on the above short review and available literature in this research airflow in an air-conditioned room in the presence of a standing mannequin was analyzed numerically.

2. Methodology

To construct the airway model a CT-Scan image was imported and processed in the Mimics. Resolution of CT-Scan image was 512×512 and the slice increment is 1 mm in axial, 0.823 mm in sagittal and coronal direction. The computational domain in the human respiratory system extends from the nostril to trachea and it is shown in Fig. 1.

The prepared airway model was connected to a standing mannequin which was constructed in 3DMax software and the whole model located in the center of the room. The external computational domain includes the region around

*Corresponding author's email: tavakol@iaushiraz.ac.ir



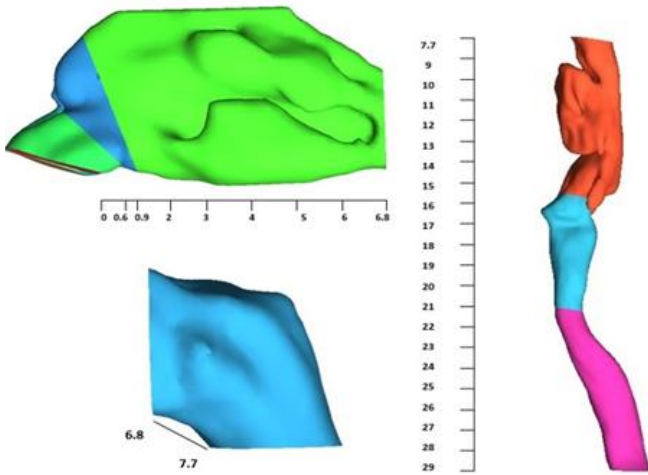


Fig. 1. Upper airway; components and dimensions

the mannequin in the room with dimensions shown in Fig. 2. Two different damper arrangements were considered; in the first mode air inlet and outlet dampers were located on the front wall and in the second mode they were located on the right side wall.

The constructed geometry was imported to the ANSYS–ICEM that is pre-processor software and unstructured tri/quadrilateral volume was generated by using the Delaunay triangulation method. Three prismatic layers were created to model boundary layer development near the walls inside the model. The computational grid in the airway passage approximately contains 7.5 million cells. To find realistic boundary condition at the airway outlet, flow inside separated airway model was simulated by solving the Navier-Stokes and continuity equations and pressure drop was calculated for various breathing rates. Steady state inhalation inlet rates of 10, 15 and 20 lit/min which resemble rest breathing and 30 and 40 lit/min which resemble physical activity were considered. In order to solve for both laminar and turbulent flow conditions, the SST $k-\omega$ transition method was used.

Steady state simulation was performed for the integrated geometry by means of $k-\omega$ SST transition model for inhalation flow rates of 15, 20 and 30 lit/min. For the inlet damper, the inlet air velocity was assumed to be 3 m/s and for outlet

damper and trachea in the airway passage, the pressure outlet boundary conditions were assumed.

3. Results and Discussion

A grid sensitivity test was accomplished with three computational domains with 6.5 million, 8.3 million and 11 million cells. For validation, the results of Xi et al. [4] for the airway system and the result of Zhang et al. [7] for air flow field in the room was used. Pressure drop in the current study is lower than previous studies due to the larger hydraulic diameter and cross-sectional area of the airway passage.

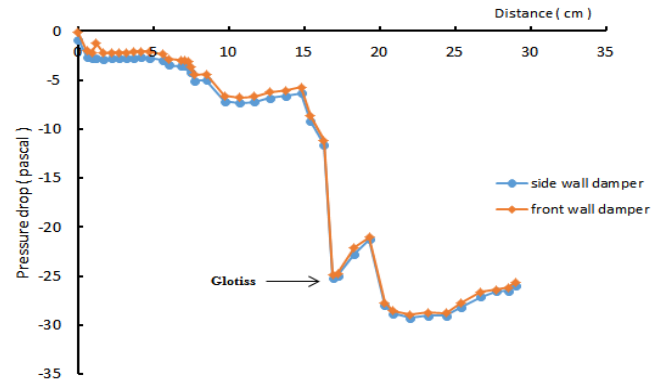


Fig. 3. Pressure drop along the airway passage for inhalation rate of 30 lit/min in the first and second mode

The maximum pressure drop is observed to occur in the glottis where hydraulic diameter suddenly decreases and the throttling process occurs. By increasing the inhalation flow rate, more pressure drop is observed in the airway passage. Fig. 3 shows the pressure distribution from nostril inlet to trachea at a flow rate of 30 lit/min for the first and second mode of dampers. Same pressure distribution can be distinguished for two modes inside the airway passage.

In Fig. 4, air velocities in the vicinity of the mannequin face are shown for three lines with 1cm distance from the mannequin face. This figure illustrates the lower air velocity near the mannequin face in the second mode of the damper which provides better comfort condition for the occupants [8].

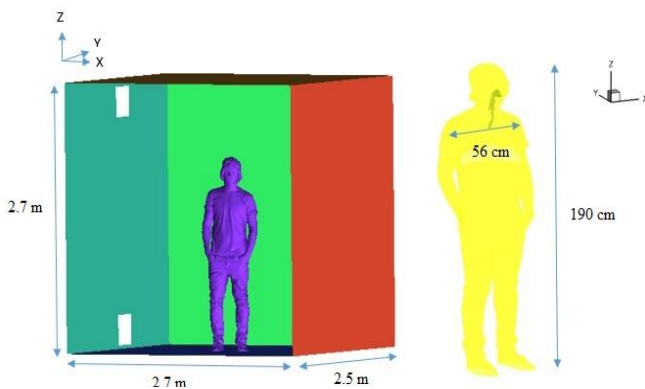


Fig. 2. Mannequin with integrated airway system in the room with dimensions.

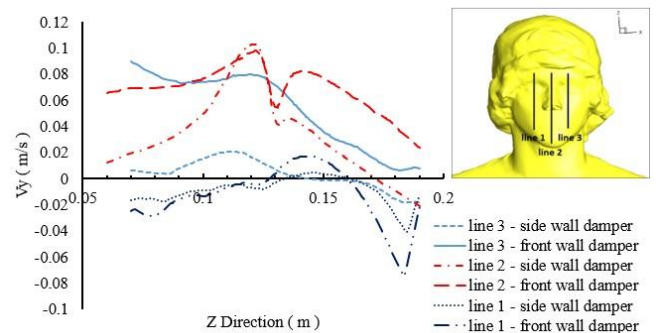


Fig. 4. Air velocity distributions near the face in the first and second mode for $Q=20$ lit/min

4. Conclusion

In this study, the air flow field around a mannequin model with the attached respiratory system inside a room at various inhalation rates was investigated numerically. By increasing inhalation flow rate pressure drop in the airway passage increases. The maximum pressure drop along the airway is observed to occur near the glottis.

In addition, according to the results for velocity distribution, the second mode of air-conditioning dampers is preferable to provide better comfort for occupants.

References

- [1] Y. Liu, E.A. Matida, J. Gu, M.R. Johnson, Numerical simulation of aerosol deposition in a 3-D human nasal cavity using RANS, RANS/EIM, and LES, *Journal of aerosol science*, 38(7) (2007) 683-700.
- [2] Y.-S. Cheng, Y. Yamada, H.-C. Yeh, D.L. Swift, Diffusional deposition of ultrafine aerosols in a human nasal cast, *Journal of Aerosol Science*, 19(6) (1988) 741-751.
- [3] J. Wen, K. Inthavong, J. Tu, S. Wang, Numerical simulations for detailed airflow dynamics in a human nasal cavity, *Respiratory physiology & neurobiology*, 161(2) (2008) 125-135.
- [4] J. Xi, A. Berlinski, Y. Zhou, B. Greenberg, X. Ou, Breathing resistance and ultrafine particle deposition in nasal-laryngeal airways of a newborn, an infant, a child, and an adult, *Annals of biomedical engineering*, 40(12) (2012) 2579-2595.
- [5] D. Rim, A. Novoselac, Transport of particulate and gaseous pollutants in the vicinity of a human body, *Building and Environment*, 44(9) (2009) 1840-1849.
- [6] C.M. King Se, K. Inthavong, J. Tu, Inhalability of micron particles through the nose and mouth, *Inhalation toxicology*, 22(4) (2010) 287-300.
- [7] T.T. Zhang, H. Li, S. Wang, Inversely tracking indoor airborne particles to locate their release sources, *Atmospheric environment*, 55 (2012) 328-338.
- [8] ASHRAE Standard, 55 (2010), Thermal environmental conditions for human occupancy, (2010).

